Proc. Natl. Acad. Sci. USA
Vol. 89, pp. 10046–10050, November 1992
Biochemistry

Hepatitis B virus capsid particles are assembled from core-protein dimer precursors

(*Xenopus* oocytes/SP6 RNA/viral assembly/disulfide bonds/protein–protein interactions)

SILIANG ZHOU* AND DAVID N. STANDRING*†‡

*Hormone Research Institute and †Department of Biochemistry and Biophysics, University of California, San Francisco, CA 94143-0534

Communicated by Rudi Schmid, August 3, 1992

ABSTRACT **Our studies on the assembly of hepatitis B virus capsids or core particles in *Xenopus* oocytes have demonstrated that unassembled p21.5 core proteins ("free p21.5") provide a pool of low-molecular-mass precursors for core-particle assembly. Here we have characterized this material. Free p21.5 sedimented through gradients of 3–25% sucrose (wt/vol) as a single protein species of ≈40 kDa, corresponding to a p21.5 dimer. On nonreducing SDS/polyacrylamide gels, free p21.5 migrated as disulfide-linked p21.5 dimeric species of 35 and 37 kDa. Truncated core proteins lacking most or all of the 36-amino acid protamine region at the p21.5 carboxyl terminus were also found to behave as disulfide-linked dimers with appropriately reduced molecular masses. Our experiments failed to reveal monomeric core proteins or stable intermediates between dimers and capsids along the assembly pathway. We conclude that hepatitis B virus core particles are most likely assembled by aggregating 90 (or possibly 180) disulfide-linked p21.5 dimers. We discuss similarities between the assembly of hepatitis B virus capsids and simple T=3 plant virus and bacteriophage structures.**

In the 28-nm spherical nucleocapsid, or core particle, of hepatitis B virus (HBV), the HBV genome resides inside a capsid shell assembled from a single 21.5-kDa viral capsid or core protein (p21.5). Electron micrographs (1) reveal that the HBV capsid surface is organized into a T=3 icosahedral lattice with ≈180 p21.5 subunits but give little information about the pathway by which capsids are assembled because the p21.5 subunits are not organized into the distinctive capsomer substructures often seen in animal virus nucleocapsids (2). Biochemical studies of p21.5 have not been much more informative (for review of the properties of p21.5, see ref. 3). Most of the first 149 residues of p21.5 are required for assembly of capsid shells in *Escherichia coli* (4, 5). Multiple disulfide bonds reportedly fuse p21.5 capsid subunits into a covalent lattice that includes at least some p21.5 dimers (4, 6), but the implications of these observations for HBV capsid assembly are unclear.

Recently, we reconstituted HBV capsid assembly in *Xenopus* oocytes programmed with a synthetic p21.5 mRNA (7, 8) and showed that a stable, nonparticulate form of p21.5 ("free p21.5") provides a pool of precursors, or assembly intermediates, for capsid assembly (8). In this report, we show that free p21.5 consists mainly of disulfide-linked p21.5 dimers.

MATERIALS AND METHODS

Plasmids and RNAs. Plasmid pSP64T-C (7, 8) encodes wild-type p21.5; plasmids Δ-157 and Δ-149 (7), respectively, encode p18, with the first 157 and last two (Gln-Cys) p21.5 residues, and p17, which is truncated to p21.5 residue Val-149. *Sal* I-linearized plasmids were used to generate capped SP6 RNAs (9).

Oocyte Methodology. Procedures for handling and injecting oocytes have been described (8). Batches of ≈20 oocytes were labeled within 3 hr of injection by transfer to modified Barth's medium (300 μl) containing antibiotics and 0.5–2 mCi per ml of [^{35}S]methionine and [^{35}S]cysteine (Expre^{35}S^{35}S, NEN) and homogenized 24–48 hr later in phosphate-buffered saline (≈15 μl per oocyte). The lysate was immediately clarified by low-speed centrifugation (Eppendorf, 15,000 × g, 10 min), and 100-μl samples were subjected to size fractionation.

Sizing Gradients. Gradients (1.2 ml) of 3–25% sucrose (wt/vol) were formed by layering steps (200 μl) of 3, 5, 10, 15, 20, and 25% sucrose in TNE (50 mM Tris·HCl, pH 7.5/100 mM NaCl/1 mM EDTA) and immediately loaded with sample (100 μl) and spun at 55,000 rpm (265,000 × *g*) for 4 hr in a TL 100 centrifuge (Beckman) using a TLS 55 swinging-bucket rotor. The gradients were then fractionated from the top (14 × 95 μl) and analyzed as described below.

Gradients were calibrated by using mixtures of the following protein standards (10 μg each in 100-μl final volume): carbonic anhydrase, serum albumin, sweet potato β-amylase, and apoferritin (Sigma), with molecular masses (supplied by the manufacturer) of 29, 66, 206, and 440 kDa, respectively. After centrifugation, 10-μl fraction samples were boiled with 10 μl of Laemmli sample buffer and resolved by discontinuous SDS/15% PAGE. Proteins were stained with Coomassie blue.

Analysis of Core Proteins by Reducing and Nonreducing SDS/PAGE. ^{35}S-labeled core proteins were immunoprecipitated from ≈25 μl of each gradient fraction with a rabbit anti-core antiserum (DAKO, Santa Barbara, CA) as described (10). Immune complexes were collected with Pansorbin (Calbiochem). For reducing SDS/PAGE, core proteins were released by boiling for 7 min in sample buffer containing 2-mercaptoethanol and analyzed on 15% polyacrylamide gels. For nonreducing SDS/PAGE, samples were heated in sample buffer without 2-mercaptoethanol for 5 min at 65°C and then at 5 min at 100°C and resolved on 10% polyacrylamide gels. Prestained protein markers (BRL) provided size standards.

RESULTS

Sizing of Marker Proteins and Free p21.5 on Sucrose Gradients. We had demonstrated (7, 8) that p21.5 expression in oocytes generates both nonparticulate (free p21.5) and capsid particle forms of p21.5 that can be resolved on 10–60% sucrose gradients. Pulse–chase experiments (8) revealed that free p21.5 constitutes the precursor to HBV capsids and showed that essentially all p21.5 could be chased into cap-

The publication costs of this article were defrayed in part by page charge payment. This article must therefore be hereby marked "*advertisement*" in accordance with 18 U.S.C. §1734 solely to indicate this fact.

Abbreviation: HBV, hepatitis B virus.

‡To whom reprint requests should be addressed at *.

sids, providing that the p21.5 concentration was sufficiently high. To characterize this free p21.5, we examined its size on minigradients of 3–25% sucrose (Fig. 1).

Gradients were calibrated with a mixture (10 μg each) of carbonic anhydrase (p29), serum albumin (p66), and sweet potato β-amylase (p206) size standards. The marker proteins in the gradient fractions were analyzed by SDS/PAGE and visualized with Coomassie blue (Fig. 1*A*; note that SDS dissociates p206 into 4 ≈50-kDa subunits). Resolution of the marker proteins is evident, with p29 in fractions 2–10 (lanes 2–10), p66 in fractions 5–11 (lanes 5–11), and p206 in fractions 10–14 (lanes 10–14).

For the analysis of free p21.5, oocytes were homogenized in phosphate-buffered saline without nonionic detergent; to further minimize disruption of any p21.5 multimers, the lysates were not frozen. Clarified lysate (≈six oocytes) was size-fractionated in parallel to the size markers. The ^{35}S-labeled p21.5 immunoprecipitated from one-third of each fraction was analyzed by reducing SDS/PAGE. The autoradiogram (Fig. 1*B*) revealed ^{35}S-labeled p21.5 in two regions of the gradient; a free p21.5 peak in fractions 3–10 (lanes 3–10) and a strong band of p21.5 capsids (molecular mass, ≈5 million Da) in the last fraction (lane 14). Control immunoprecipitation experiments (data not shown) revealed that clarification of extracts by low-speed centrifugation resulted in minimal p21.5 losses.

The overall shape of the free ^{35}S-labeled p21.5 gradient profile is very similar to those of the p29 and p66 markers (Fig. 1*A*), as is evident from a cut-and-paste comparison of the three profiles (Fig. 2*A*, a–c). This result implies that free p21.5 (*b*) is mainly a single protein species. The peak of free p21.5 is shifted roughly one fraction down the gradient relative to p29 (*c*) and up two fractions relative to p66 (*a*); the

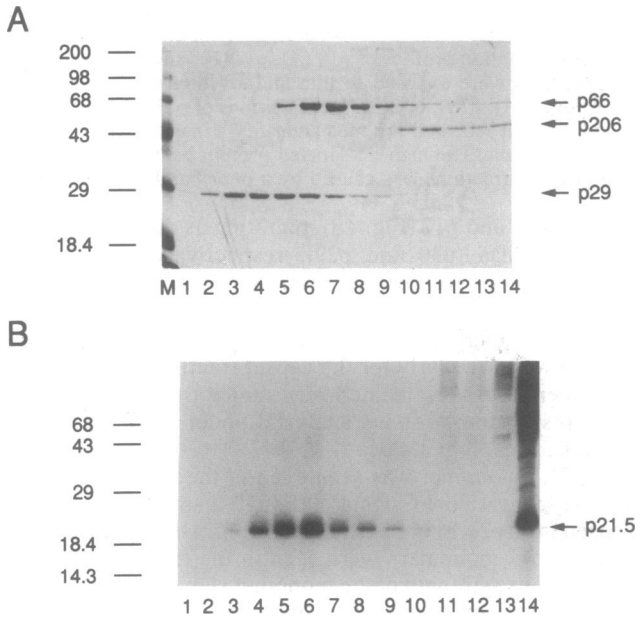

FIG. 1. Sedimentation of marker proteins and p21.5 on sucrose gradients. Fractionation on parallel 3–25% sucrose gradients of marker proteins—p29 carbonic anhydrase, p66 serum albumin, and p206 sweet potato β-amylase (*A*)—and ^{35}S-labeled p21.5 species (*B*). The 14 gradient fractions were sampled by SDS/PAGE with a 10% (*A*) or 15% (*B*) gel and are shown in order from top (lane 1) to bottom (lane 14) of gradient. Marker proteins were stained with Coomassie blue; immunoprecipitated ^{35}S-labeled p21.5 was detected by 3-day exposure to x-ray film at −70°C. Positions of the p29, p66, and p206 marker proteins are indicated at right of *A*, and the position of p21.5 is indicated at right of *B*. Note that p206 dissociates into ≈50-kDa subunits upon SDS treatment. Positions of electrophoretic molecular mass markers (*A*, lane M) are shown at left in kDa.

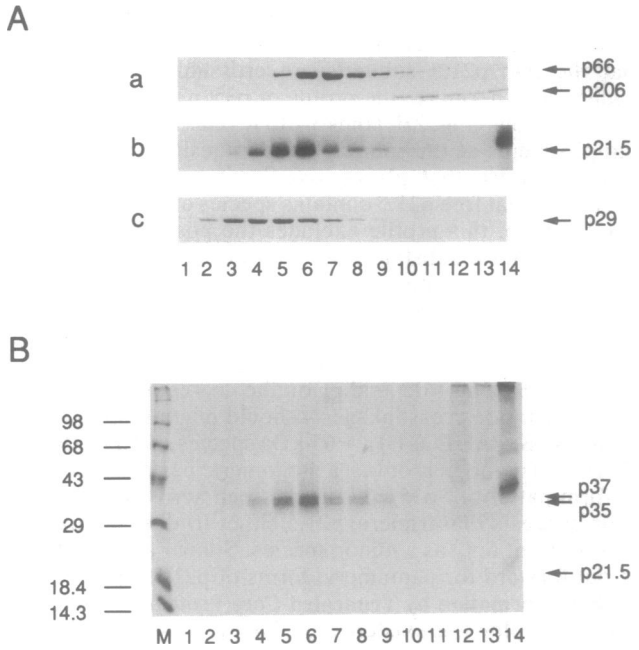

FIG. 2. Size fractionation of free p21.5 under reducing and nonreducing conditions. (*A*) Cut-and-paste comparison showing alignment of the sedimentation profiles for p66 and p206 (*a*); ^{35}S-labeled p21.5 (*b*); and p29 (*c*). See Fig. 1 for details. (*B*) Analysis of size-fractionated ^{35}S-labeled p21.5 species by SDS/PAGE under nonreducing conditions. Details can be found in the legend to Fig. 1 and in text. Autoradiography was for 3 days at −70°C, and the fractions are arranged from top (lane 1) to bottom (lane 14) of gradient; lane M (*B*) shows radioactive protein size markers in kDa at left. Positions of p29, p66, and p206 marker proteins and of p21.5, p35, and p37 capsid protein species are shown at right.

three main fractions for each species being 3–5 for p29, 4–6 for p21.5, and 6–8 for p66. These data suggest a molecular mass of ≈40 kDa for free p21.5 (slightly closer to p29 than to p66).

The most straightforward interpretation of this result is that free p21.5 is mostly p21.5 dimers (predicted molecular mass, 43 kDa); the data are less compatible with p21.5 monomers (which should migrate with a peak around fractions 2–4), or trimers with an anticipated profile similar to p66. Free p21.5 is unlikely to be a heterogeneous mixture of p21.5 multimers (this would yield a much broader gradient peak), although the possibility that free p21.5 contains small amounts of additional p21.5 species cannot be excluded. Additional lines of evidence presented below support the view that the dimer is, indeed, the fundamental building block for core particles.

p21.5 Dimers Are Disulfide-Linked. Because HBV capsids assembled in *E. coli* contain disulfide-linked p21.5 molecules, including dimers (4), we next analyzed free p21.5 by SDS/PAGE in the absence of reduction (Fig. 2*B*) to determine whether this species includes disulfide-linked dimers of p21.5.

Because the free ^{35}S-labeled p21.5 used for this analysis was immunoprecipitated from a further aliquot of the fractions derived from the sizing gradient shown in Fig. 1*A*, the gradient profiles obtained by reducing (Fig. 1*B* or 2*A*, *b*) or nonreducing SDS/PAGE (Fig. 2*B*) can be compared directly and are clearly similar. However, unreduced p21.5 migrated on gels as almost equal amounts of 35 and 37 kDa species (p35 and p37), which presumably represent disulfide-linked dimeric forms of p21.5; p35 and p37 were not immunoprecipitated from control oocytes gradients (data not shown). Whether p35 and p37 represent two distinct dimer species is unclear; they could arise artifactually (e.g., during sample preparation for electrophoresis).

Thus, the nonreducing SDS/PAGE data confirm that the capsid assembly intermediates are p21.5 dimers and indicate that the two p21.5 subunits are crosslinked by disulfide bridges. Furthermore, the profile of p35/p37 within the free p21.5 fractions (Fig. 2*B*, lanes 3–10) reveals the same two p35 and p37 bands at the same relative intensities in each fraction—a pattern that places significant constraints on the possibility that free p21.5 contains species other than dimers. For example, this profile excludes the possibility that free p21.5 includes a substantial amount of cryptic p21.5 monomer because this species should become apparent in this analysis as a 21.5-kDa band with a peak of activity in fractions 2–4. Similarly, if free p21.5 included a significant amount of p21.5 trimer, this species should band with a peak in fractions 6–8 (like p66) and—depending on the degree of the intermolecular disulfide crosslinkages—should migrate upon nonreducing SDS/PAGE as (*i*) a ≈65-kDa species, (*ii*) a mixture of dimer plus monomer, or (*iii*) a monomeric p21.5. The simple, uniform pattern of p35/p37 dimers seen across the gradient again suggests that trimeric p21.5 either (*i*) does not exist or (*ii*) is present only as a minor species. Similar arguments can be put forward for pentameric forms of p21.5.

Dimer Formation by Truncated Core Proteins. A third line of evidence for the existence of dimeric-assembly intermediates for HBV capsids was obtained by using two mutant core proteins truncated to different endpoints within the 36-amino acid protamine region (residues 150–185), which is fully dispensible for capsid assembly (4, 5). Mutant Δ-149 encodes a 17-kDa polypeptide (p17) that is contiguous with p21.5 up to Val-149 but lacks the entire protamine region. Mutant Δ-157 encodes a protein of 18 kDa (p18) that contains the entire p21.5 sequence up to Ser-157 plus the final two p21.5 residues (Gln-184–Cys-185). Dimers assembled from these mutant core proteins were expected to exhibit a detectable reduction in molecular mass (≈8 kDa) compared to wild-type p21.5.

Lysates from oocytes expressing these proteins were fractionated on parallel sucrose gradients and analyzed by reducing SDS/PAGE as described above. For Δ-157 (Fig. 3*A*), the autoradiogram showed an intense band of p18 capsids in the final fraction (lane 14) and a peak of free p18 in fractions 2–10 (lanes 2–10); Δ-149 (Fig. 3*B*) displayed a weak band of p17 capsids (lane 14) and a substantial amount of free p17 (lanes 2–10); p21.5 (Fig. 3*C*) displayed p21.5 capsids in fraction 14, and free p21.5 localized mainly in fractions 3–11. The profiles of the free p18 and p17 species were clearly shifted at least one to two fractions higher up the gradient relative to free p21.5, indicating that these species are, indeed, of lower molecular mass than p21.5 dimers. The fraction containing the highest amount of each species was as follows (with the three main fractions given in parentheses); fraction 5 for p18 (4–6), fraction 5 for p17 (3–5), and fraction 6 for p21.5 (5–7). This size difference was confirmed by mixing lysates of p17 and p21.5 and subjecting them to sedimentation; after immunoprecipitation and autoradiography, the free p17 peak was found shifted one fraction up the gradient compared with the free p21.5 peak (data not shown).

Comparison among the sedimentation profiles of p17, p18, p21.5, and the protein molecular mass standards resolved on a parallel gradient (almost identical to that seen in Fig. 1*A*; data not shown) indicates that free p17 shows the same distribution as the p29 carbonic anhydrase standard (indicating a mass of ≈29 kDa), whereas free p18 is slightly larger than p29 or free p17 but smaller than the p21.5 dimer, consistent with molecular masses of 30–35 kDa. Thus, free p17 and free p18 appear to behave as core-protein dimers.

Nonreducing SDS/PAGE Analysis of Mutant Dimers. The gradients described above again provided the source of p18, p17, and p21.5 dimers for analysis by nonreducing SDS/PAGE (Fig. 4 *A–C*). The autoradiograms showed unreduced

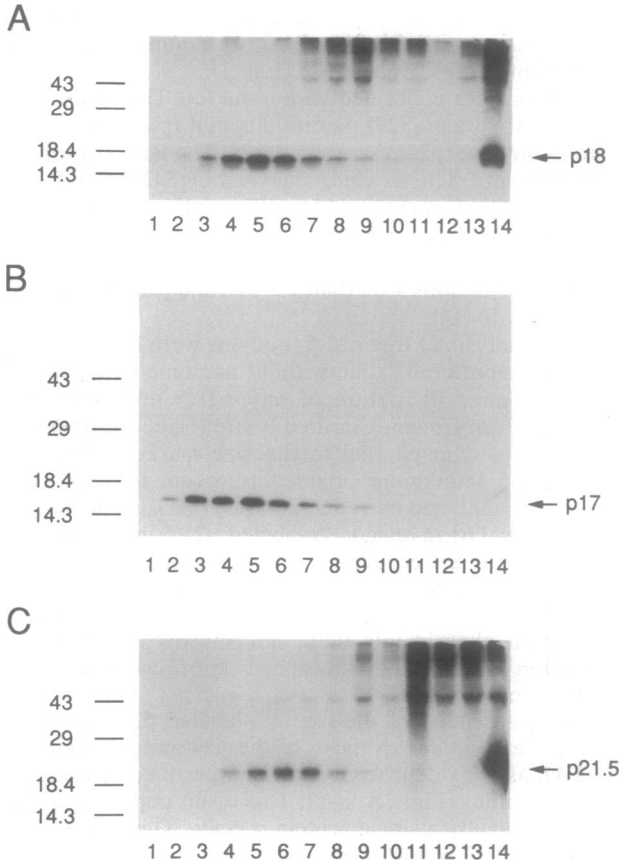

FIG. 3. Sizing of free p18, p17, and p21.5 proteins. Sedimentation, immunoprecipitation, and nonreducing SDS/PAGE analysis of ^{35}S-labeled core proteins were done as described. Autoradiograms show sedimentation profiles of p18 (*A*), p17 (*B*), and p21.5 (*C*) core proteins. Gels were exposed to film and an intensifying screen at −70°C for 20 (*A*), 4 (*B*), or 24 (*C*) hr. Positions of p17, p18, and p21.5 are indicated at left, and the molecular-mass markers (in kDa) are indicated at right. The high ^{35}S-labeled protein background seen in some gradient fractions was caused by a poor batch of Pansorbin.

p18 (Fig. 4*A*) and p17 (Fig. 4*B*) migrating as diffuse bands of 30 and 29 kDa (p30 and p29), respectively (with minor secondary bands visible in some lanes); p21.5 (Fig. 4*C*) again yielded p35 and p37 species (cf., Fig. 2*B*). Recovery of the core proteins under nonreducing conditions generally appeared low, particularly for the capsid fraction (lane 14), but the gradient profiles remained very similar overall to those of the corresponding proteins analyzed under reducing conditions (cf., Figs. 3 and 4).

No p21.5 monomer was seen even in the free p21.5 lanes with the highest dimer signal, although a small amount was released from p21.5 core particles. In contrast, small amounts of p18 or p17 monomers were seen in the free core-protein lanes. Because strength of the monomer signal reflects that of the dimer in each case, these "monomers" have probably arisen after fractionation and could represent, for example, a small percentage of the p17 and p18 dimers in which disulfides failed to form. Species of 43 and 60 kDa (corresponding to trimers and tetramers), seen in the p18 capsid lane (Fig. 4*A*, lane 14) and faintly in the p18 dimer lanes, also appear to arise after fractionation.

Absence of Detectable Higher-Molecular-Weight Assembly Intermediates. The preceding evidence points to p21.5 dimers being the main assembly intermediates for HBV capsids. To look more carefully for larger intermediates, we centrifuged ^{35}S-labeled p21.5 through a 3–25% sucrose gradient for 2 hr rather than the normal 4 hr. The marker proteins p66 and

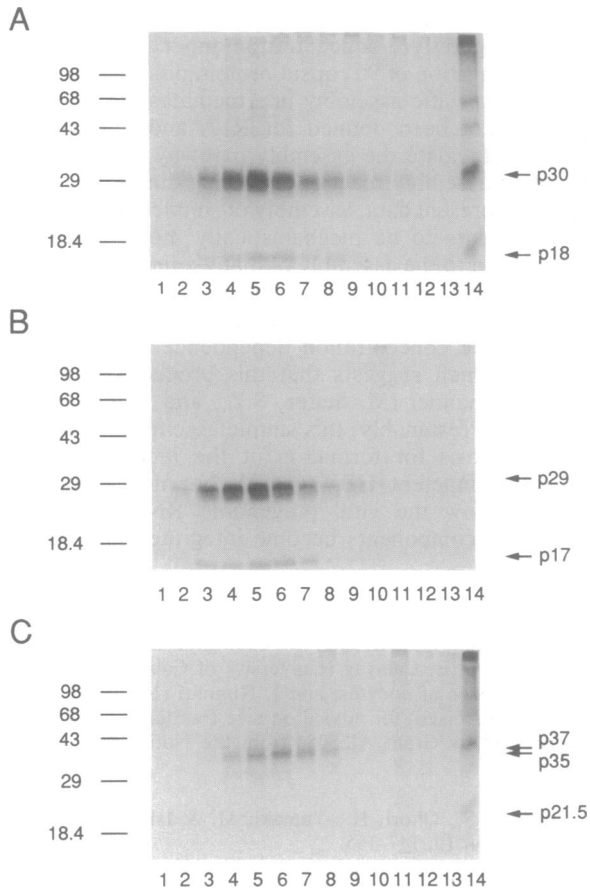

FIG. 4. Nonreducing analysis of p18, p17, and p21.5 dimers. This experiment is identical in every detail to the one of Fig. 3, except the immunoprecipitated p18 (*A*), p17 (*B*), and p21.5 (*C*) core proteins were analyzed by nonreducing SDS/PAGE, and the gels were exposed to film for 6 days at 22°C. Numbers of gradient fractions are shown below *A–C*, positions of prestained electrophoretic markers are shown at left (in kDa), and positions of p17, p18, and p21.5 monomers and p29, p30, and p35/37 dimers are shown at right.

p206, along with 440-kDa apoferritin (p440), were resolved on a parallel gradient along with an authentic sample of purified recombinant p17 (Δ-149) capsids derived from *E. coli*. After SDS/PAGE, the marker proteins were stained with Coomassie blue (Fig. 5*A*), and the immunoprecipitated ^{35}S-labeled p21.5 species were detected by autoradiography (Fig. 5*B*).

p440 (sedimentation coefficient, ≈17S) was found distributed through fractions 9–14 with the bulk in fractions 10 and 11 (SDS dissociates apoferritin into ≈24 heterogeneous subunits of ≈19 kDa); p206 (sedimentation coefficient, ≈8.9S) was seen in fractions 5–11, with 6 and 7 being the main fractions; and p66 localized to the first 10 fractions, with the most intense staining in fraction 4. The p17 capsids sedimented as a heavy protein band seen only in fraction 14. For p21.5 (Fig. 5*B*) a peak of capsids was seen in fraction 14, and free p21.5 was seen in fractions 1–7; fractions 3 and 4 were the peak free p21.5 fractions. These data are again consistent with free p21.5 being slightly smaller than p66, and analysis of the free p21.5 by nonreducing SDS/PAGE confirmed its dimeric structure (data not shown).

Other than dimers, the data reveal no detectable core-particle assembly intermediates between ≈40 and >440 kDa; assembly intermediates much beyond 440 kDa in size should be resolved on conventional 10–60% sucrose gradients but are not detected (8).

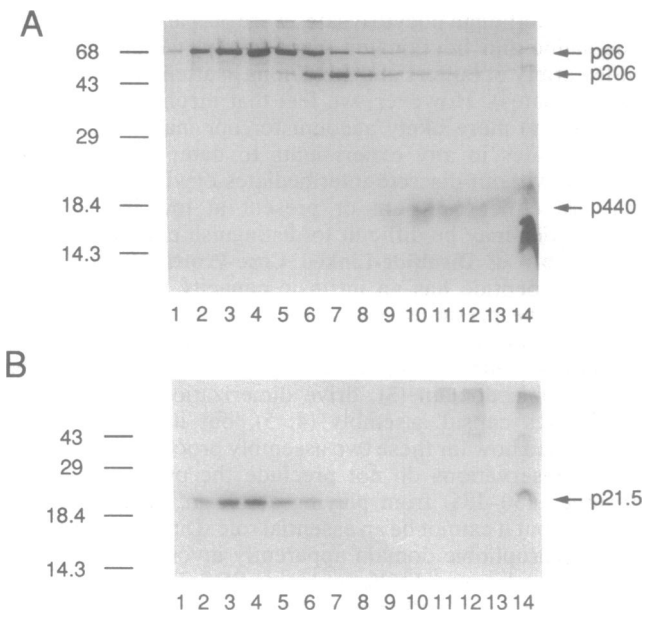

FIG. 5. Absence of higher p21.5 multimers. Molecular-mass standards (*A*) and ^{35}S-labeled p21.5 species (*B*) were fractionated by 2-hr centrifugation through minigradients of 3–25% sucrose and analyzed as described in text and the legend to Fig. 1. Positions of Coomassie-blue stained serum albumin (p66), β-amylase (p206), and apoferritin (p440) are indicated at right of *B*; the thick band of ≈17-kDa protein seen only in lane 14 shows the sedimentation of recombinant p17 capsids. Immunoprecipitated ^{35}S-labeled p21.5 (*B*) was detected by autoradiography (20 hr at −70°C). Sizes of prestained marker proteins (in kDa) are shown at left.

DISCUSSION

In this report we have shown that nonparticulate free p21.5 is composed mainly of disulfide cross-linked dimers of p21.5. Although dimerization of hepadnaviral core proteins is well-documented (4, 6, 11, 12), the relationship between dimerization and capsid assembly is unclear. Our study now provides clear evidence that dimers are the building blocks for core-particle assembly.

Free (Unassembled) Core Proteins Are Mainly Dimers. The free (i.e., nonparticulate) p21.5 found in oocytes sedimented through 3–25% sucrose sizing gradients as a protein with an apparent molecular mass of ≈40 kDa and migrated as species of 35 and 37 kDa (p35 and p37) upon nonreducing SDS/PAGE. The unassembled forms of carboxyl-terminally truncated p17 and p18 core proteins behaved as species of ≈29–35 kDa by these two tests. These data suggest that free core-protein species comprise mainly dimers that apparently contain little or no tightly bound RNA (bound RNA should significantly increase mass).

Pulse–chase experiments (8) had shown that free p21.5 acts as the precursor pool for HBV capsids in *Xenopus* oocytes. We can, therefore, now conclude that p21.5 dimers are the major assembly units for HBV capsids. We propose, based on estimates of 180 p21.5 subunits per capsid (1), that HBV capsids are assembled by aggregating 90 p21.5 dimers (if the 180 morphological units seen in micrographs represent p21.5 dimers, the HBV capsid would contain 360 p21.5 subunits). Recent biochemical studies are consistent with the idea that capsids contain p21.5 dimers (4, 6).

Our data shed little direct light on the pathway by which p21.5 dimers assemble into HBV capsids because we were unable to identify discrete intermediates along this pathway. This absence of such intermediates could reflect experimental causes; their detection may be hampered by the low resolution of our sizing gradients, or these species may be

unstable (although oocyte lysates were prepared in detergent-free saline and fractionated immediately, we did not try a wide variety of buffers and metal ions in attempts to stabilize intermediates). However, we feel that mechanistic reasons (see below) more likely account for our inability to detect intermediates in any experiments to date; assembly may proceed without discrete intermediates or via intermediates that are either transient or present at low levels. Such possibilities may be difficult to distinguish experimentally.

Assembly of Disulfide-Linked Core-Protein Dimers. The core polypeptide has an intrinsic capacity to dimerize. In oocytes, the presumed monomer–dimer equilibrium apparently lies far to the dimer side under our experimental conditions. Our data reveal that p21.5 residues 1–149, the hydrophobic domain (3), drive dimerization. This domain also drives capsid assembly (4, 5), but it remains to be ascertained how far these two assembly processes are linked. These observations do not preclude the protamine region (residues 150–185) from playing a role in either assembly process, but it cannot be an essential role. Dimerization of the p21.5 hydrophobic domain apparently involves a structural compaction because by nonreducing SDS/PAGE, dimers of p17, p18, and p21.5 all appeared ≈6 kDa smaller than would be predicted from the monomer size.

Because the p17, p18, and p21.5 dimers were all stabilized by disulfide bonds (at least upon isolation), at least one of the three cysteine residues in the hydrophobic domain (Cys-48, Cys-61, or Cys-107) participates in disulfides. However, a recent mutational analysis (13) of these cysteine residues reveals that they do contribute to the stability of these structures but are not required for either dimer or capsid formation.

Intriguingly, our nonreducing SDS/PAGE data hint that equal populations of p35 and p37 dimers might be used to assemble HBV capsids; however, the natures of p35 and p37 remain unknown, and we have not excluded the possibility that one of these species is an electrophoretic artefact rather than a true *in vivo* product.

Possible Assembly Pathways for HBV Capsids. Closely related icosahedral virus structures can assemble by different pathways. We are now in a position to begin to analyze how HBV capsid assembly compares with the assembly of other viral structures.

Among animal RNA viruses, the assembly of picornaviruses is particularly well studied (2, 14). Picornaviruses elaborate four capsid proteins (VP1, VP2, VP3, and VP4) that initially assemble into discrete 5S protomers of 80–100 kDa. Five protomers then aggregate into stable pentameric 13–14S structures of ≈400 kDa, and 12 pentamers ultimately combine to create the nucleocapsid. Thus, picornavirus assembly proceeds in an ordered pathway involving stable pentameric intermediates. The assembly of the simian virus 40 (15) and polyomavirus (16) DNA viruses also depends on pentameric intermediates. Polyomavirus VP1 assembles into stable pentamers when expressed in *E. coli* (16).

In contrast, the T=3 icosahedral structures of unenveloped plant viruses, such as tomato bushy stunt virus (15), or bacteriophages, such as R17 (17), are assembled by a quite different pathway with building blocks composed of dimers of a single capsid protein. Assembly of the R17 bacteriophage is a highly cooperative, concentration-dependent process involving aggregation of 90 capsid protein dimers (17). To our knowledge, specific assembly intermediates higher than dimers have not been defined for R17, and it is generally difficult to elucidate the assembly pathway for this type of cooperative assembly reaction involving dimers.

From our present data, assembly of simple HBV capsids in oocytes appears to be mechanistically more akin to R17 assembly than to the assembly of many animal viruses. This conclusion is supported by (*i*) the preference for dimeric rather than pentameric p21.5 intermediates and (*ii*) a recent analysis of the concentration dependence of HBV capsid formation, which suggests that this proceeds in a highly cooperative manner (M. Seifer, S.Z., and D.N.S., unpublished data). Presumably, this simple assembly scheme also provides a basis for formation of the more complicated replication-competent HBV capsid, but it remains to be determined how the viral pregenome RNA and reverse transcriptase components become integrated into this process.

We thank T. Hatton and M. Seifer for communicating their unpublished results and M. Seifer for reading this manuscript. We are grateful to M. C. B. Calayag (University of California, San Francisco) for supplies of oocytes, and J. Nunnari (University of California, San Francisco) for advice on size fractionation. This work was supported by Grant AI25056 from the National Institutes of Health.

1. Onodera, S., Ohori, H., Yamaki, M. & Ishida, N. (1982) *J. Med. Virol.* **10**, 147–155.
2. Rossmann, M. G. & Johnson, J. E. (1989) *Annu. Rev. Biochem.* **58**, 533–537.
3. Standring, D. N. (1991) in *Molecular Biology of the Hepatitis B Virus*, ed. McLachlan, A. (CRC, Boca Raton, FL), pp. 145–169.
4. Gallina, A., Bonelli, F., Zentilin, L., Rindi, G., Muttini, M. & Milanesi, G. (1989) *J. Virol.* **63**, 4645–4652.
5. Birnbaum, F. & Nassal, M. (1990) *J. Virol.* **64**, 3319–3330.
6. Jeng, K.-S., Hu, C.-P. & Chang, C. (1991) *J. Virol.* **65**, 3924–3927.
7. Zhou, S. L. & Standring, D. N. (1991) *J. Virol.* **65**, 5457–5464.
8. Zhou, S., Yang, S. Q. & Standring, D. N. (1992) *J. Virol.* **66**, 3086–3092.
9. Standring, D. N., Ou, J.-H. & Rutter, W. J. (1986) *Proc. Natl. Acad. Sci. USA* **83**, 9338–9342.
10. Standring, D. N., Ou, J.-H., Masiarz, F. R. & Rutter, W. J. (1988) *Proc. Natl. Acad. Sci. USA* **85**, 8405–8409.
11. Takahashi, K., Akahane, Y., Gotanda, T., Mishiro, T., Imai, M., Miyakawa, Y. & Mayumi, M. (1979) *J. Immunol.* **122**, 275–279.
12. Petit, M.-A. & Pillot, J. (1985) *J. Virol.* **53**, 543–551.
13. Zhou, S. & Standring, D. N. (1992) *J. Virol.* **66**, 5393–5398.
14. Rueckert, R. R. (1991) in *Fundamental Virology*, eds. Fields, B. N. & Knipe, D. M. (Raven, New York), pp. 409–450.
15. Harrison, S. C. (1991) in *Fundamental Virology*, eds. Fields, B. N. & Knipe, D. M. (Raven, New York), pp. 37–61.
16. Salunke, D., Caspar, D. L. D. & Garces, R. L. (1986) *Cell* **46**, 895–904.
17. Beckett, D. & Uhlenbeck, O. C. (1988) *J. Mol. Biol.* **204**, 927–938.